



Evaluation of Seismic Vulnerability of Specially Reinforced Concrete Frames (SRCF) by FEMA-P695 Method

Hamze Rouhi

Department of Civil Engineering, Semnan University, Semnan, Iran.

*Corresponding author: Hamze Rouhi; hamzerohi@yahoo.com

Received 02 February 2023;

Accepted 12 April 2023;

Published 18 April 2023

Abstract

Seismic behaviour of Special Reinforced Concrete Frame with high ductility, designed according to the 4th edition of Iranian earthquake standard 2800, in four structural models of 4, 8, 12, and 24 stories under all of earthquake records of the far-field and near-field recommended by FEMA-P695, have been evaluated by performing incremental dynamic analysis (IDA). Fragility curves are drawn for structural models. The results of this research and the evaluation of effective parameters in the evaluation of the safety margin of collapse show that the special reinforced concrete frame (SRCF) designed with the 4th edition of the 2800 standard, except for high-rise structures, has an acceptable performance against the design seismic loads and maximum credible earthquake.

Keywords: Reinforced Concrete Frame, Incremental Dynamic Analysis, Fragility, FEMA-P695.

1. Introduction

With fragility curves that show the probability of structural failure for different levels of earthquake intensity, it is possible to prioritize structures for retrofitting by determining the degree of their vulnerability. In 1980, the fragility curve was first used for nuclear power plants. It was drawn [1]. These curves were drawn by using factors of fragility such as water pressure, concrete strength, displacement and stress created in the tank shells based on different levels of maximum earthquake acceleration. After the Northridge earthquake (1994), more attention was paid to estimating the amount of damage to structures, and engineers paid more attention to predicting the amount of financial damage to structures in more severe earthquakes. In 1994, during a study on structures in the state of California, ATC-13 criteria were used to draw fragility curves [2]. In 2014 [3], Shin et al. analysed the fragility of reinforced concrete flexural frames and investigated the change in the performance of the structure due to the occurrence of the seismic sequence phenomenon.

Due to the relatively new research and studies on the seismic vulnerability of bending frames using fragility curves, this research is also part of the studies to help further studies in this field.

In this research, the group of earthquake records including 44 far-field earthquake records and 56 near-field earthquake records proposed by FEMA-P695 [4] has been used, and due to the relatively large number of earthquake records, the results are highly accurate.

2. Validation of Reinforced Concrete Frame

Choi and Park in 2011 [5] conducted a laboratory study to investigate the cyclic behavior of reinforced concrete frame. To this end, the tested three-story frame Figure 1 a) shows this frame [5]. In this research, in order to ensure the accuracy of the modelling, the numerical model of the laboratory sample was analysed in OpenSees finite element software [6]. For modeling, the nonlinear beam-column element (nonlinear Beam Column) has been used for beam and column elements with deformation control, which has the ability to include P-Δ effect and large deformations. In order to model the extensive plasticity in the elements in the program, the sections of the beam and column elements are divided into a number of fibers. Also, Concrete01 and Steel02 materials have been used to model concrete and steel reinforcements, respectively. Also, the discussion of concrete encasement of columns has been seen in the model. The numerical results obtained from cyclic loading are compared with the experimental results (Figure 1b). The values of load bearing capacity, initial stiffness determined from the experiment and the corresponding simulated model are presented in Table 1. As can be seen from Figure 1b related to the hysteresis curve of the numerical model and laboratory sample of Choi and Park and Table 1, the finite element model using OpenSees software can be used to predict the behaviour of the reinforced concrete frame with appropriate accuracy.

Table 1: Comparison of finite element analysis results [6] and Choi and Park model test [5].

Lateral load (KN)			Elastic stiffness (KN/mm)		
Test	Finite element	Ratio finite element to test	Test	Finite element	Ratio finite element to tes
190	173	0.91	6	6	1

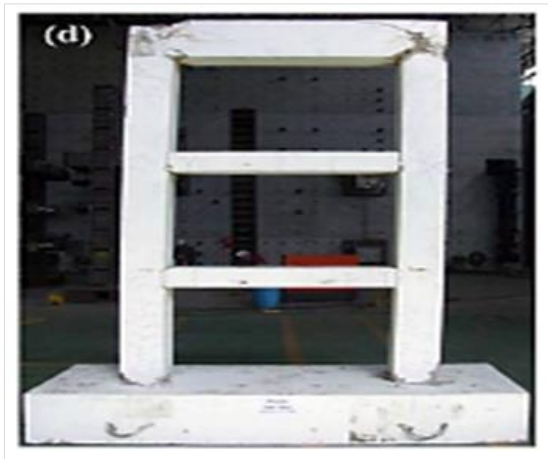


Figure 1 a. Reinforced Concrete Frame [5].

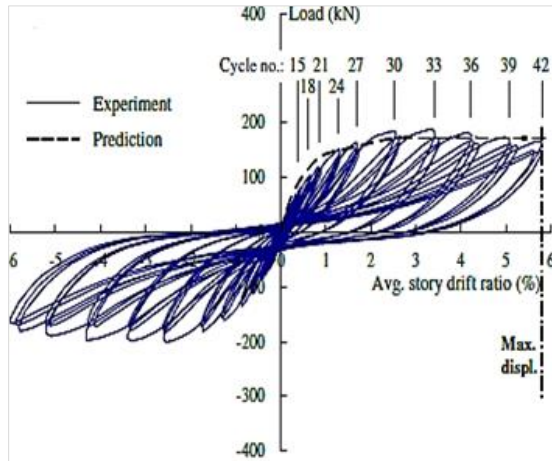


Figure 1 b. Hysteresis curve of numerical model and test [5].

3. Modelling

Regarding the classification of structural systems, some consider the height-to-dimension ratio as the criteria for classifying structures, and the height-to-dimension ratios are greater than 1.5π , between π and 1.5π , between 0.5π and π and less than 0.5π are known as high, mid, and low-rise structures respectively [7]. Therefore, in this research, four structure models of 4, 8, 12, and 24 stories with height-to-dimension ratios of 0.54, 1.09, 1.63, and 3.26 in the classification of low, mid, mid, and high-rise structures with a rectangular plan according to Figure 2a is selected with Special Reinforced Concrete Frame (SRCF). The height of the stories of the models is 3.4 m. The supports of all structures are fixed and the construction site of the structures is considered to be an area with high relative risk and soil type III. The concrete used in the C25 class

concrete structure has a characteristic strength of 250 kg/cm^2 and the rebars are of A3 type with a yield stress of 4000 kg/cm^2 . In the analysis and design of the researched structures, the 6th [8] and 9th [9] topics of the National Building Regulations and the Iran Earthquake Standard 2800, 4th edition [10] have been used.

The dead load of the stories and roof is 640 kg/m^2 , the live load of the floors and roof is 200 kg/m^2 , and the load of the surrounding walls of the floors is 600 kg/m^2 . For the real and rational design of the structures, the behavior coefficient of 7.5 was used for this system [10]. Among the models, the structural sections of the two-dimensional model of the 4-story have been presented in Figure 2b. Designed beams and columns of the 8-story, 12-story, and 24-story models also the results of modal and nonlinear analysis of models have been presented in [11].

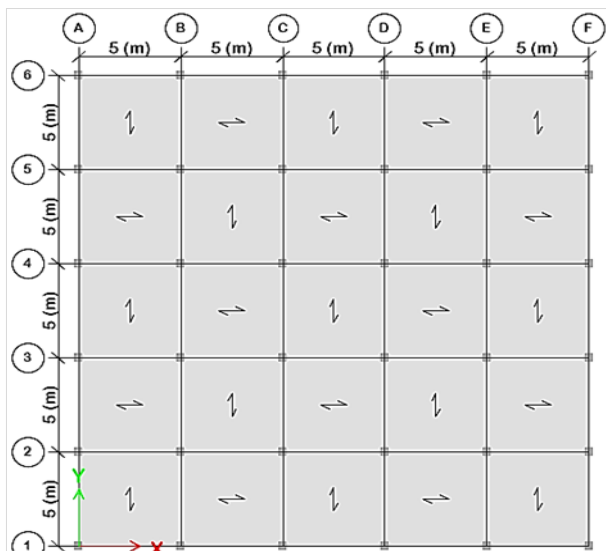


Figure 2 a. Joint plan of structural models

	B40X35	B40X35	B40X35	B40X35	B40X35
C35-8F16	B40X35 C35-8F16	B40X35 C35-8F16	B40X35 C35-8F16	B40X35 C35-8F16	B40X35 C35-8F16
C35-8F16	B40X40 C35-8F16	B40X40 C35-8F16	B40X40 C35-8F16	B40X40 C35-8F16	B40X40 C35-8F16
C40-8F16	B40X40 C40-8F16	B40X40 C40-8F16	B40X40 C40-8F16	B40X40 C40-8F16	B40X40 C40-8F16
C40-8F16	C40-8F16	C40-8F16	C40-8F16	C40-8F16	C40-8F16

Figure 2 b. structural sections of the two-dimensional model of the 4-story

4. Seismic Records used in Nonlinear Dynamic Analysis

In this research, a group of earthquake record, including the records proposed by FEMA-P695, have been used. This set of records includes 22 earthquake records of the far-field (records with a distance of more than 10 km from the fault) with two horizontal components and 28 earthquake records of the near-field (14 records of the near-field with pulse and 14 near-field records without pulse)

with two horizontal components. The models have been analysed under these records proposed by FEMA-P695.

5. Incremental Dynamic Analysis (IDA) [12]

The incremental dynamic analysis method (IDA) [12] was proposed for the first time in 2000 by Professor Cornell at Stanford University, and in 2002, it was investigated for a 20-story building during Dr. Vamvatsikos' project under the supervision of Professor Cornell. In fact, IDA is a non-linear dynamic analysis that can be used to

determine the amount of damage to the structure according to the intensity of the earthquake stimulation.

6. Results of IDA

6.1. Results of IDA for Far-Field Records

The results of the nonlinear IDA of structural models under FEMAP695 far-field records are presented in figures 3 to 6 and their failure curves in figures 7 to 10. Also, the results of the nonlinear IDA of the structural models under the near-field with pulse FEMAP695 are presented in figures 11 to 14 and their failure curves in figures 15 to 18. Figures 19 to 22 show failure curves of models under without pulse FEMAP695 near-field records.

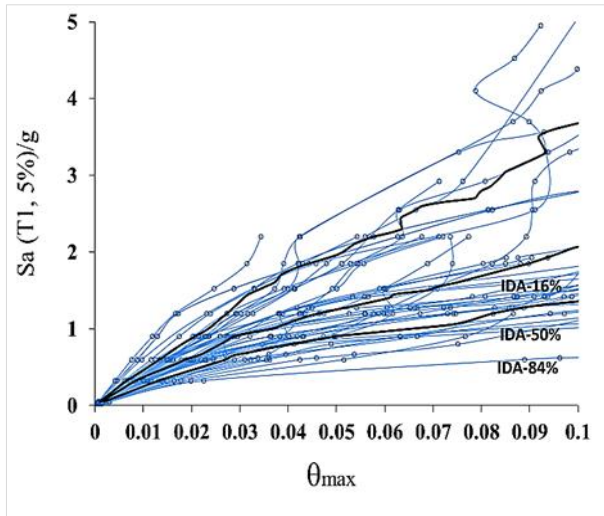


Figure 3. IDA curves of 4-story model for far-field records.

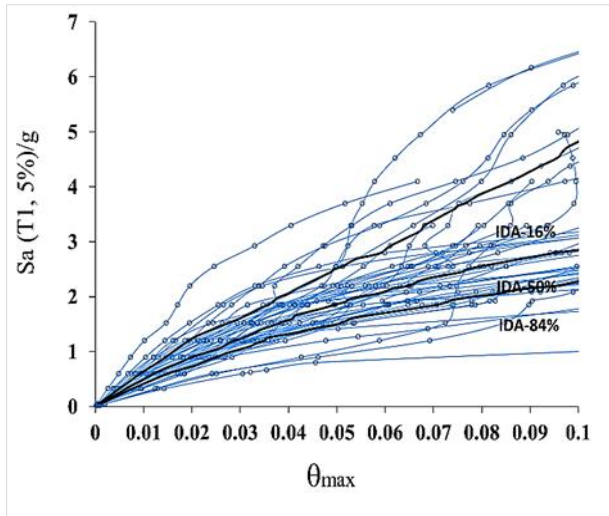


Figure 4. IDA curves of 8-story model for far-field records.

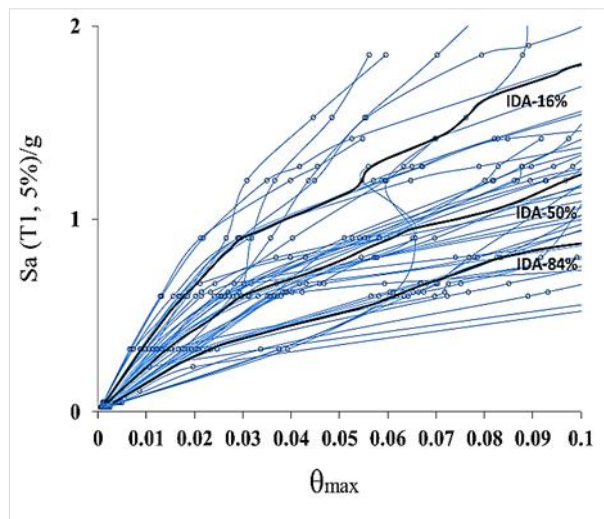


Figure 5. IDA curves of 12-story model for far-field records.

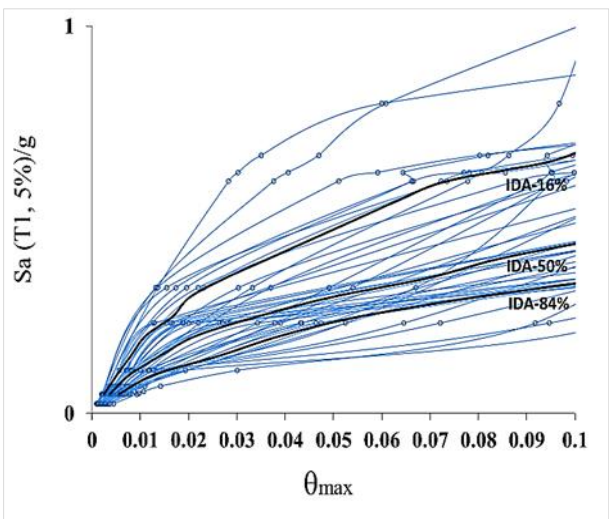


Figure 6. IDA curves of 24-story model for far-field records.

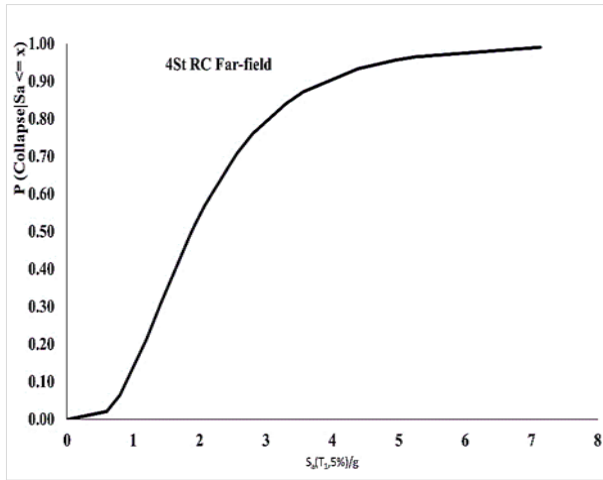


Figure 7. Fragility curves of 4-story model for far-field records.

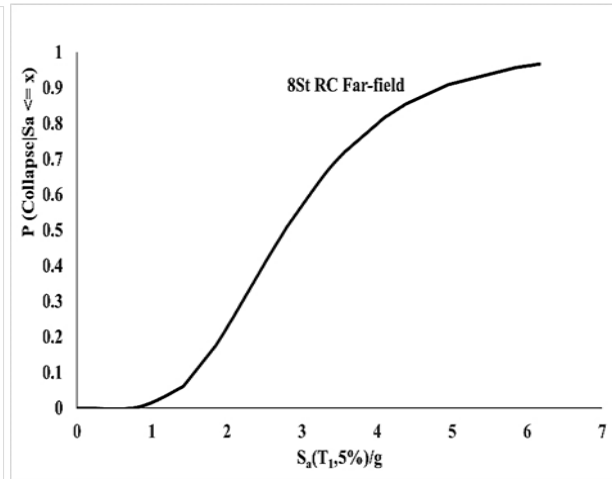


Figure 8. Fragility curves of 8-story model for far-field records.

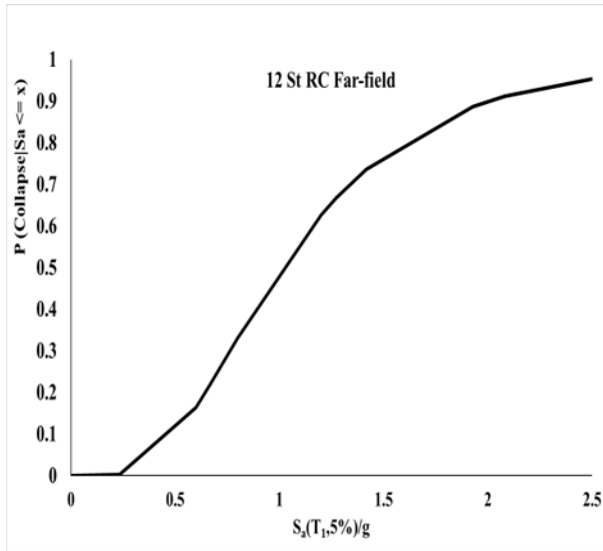


Figure 9. Fragility curves of 12-story model for far-field records.

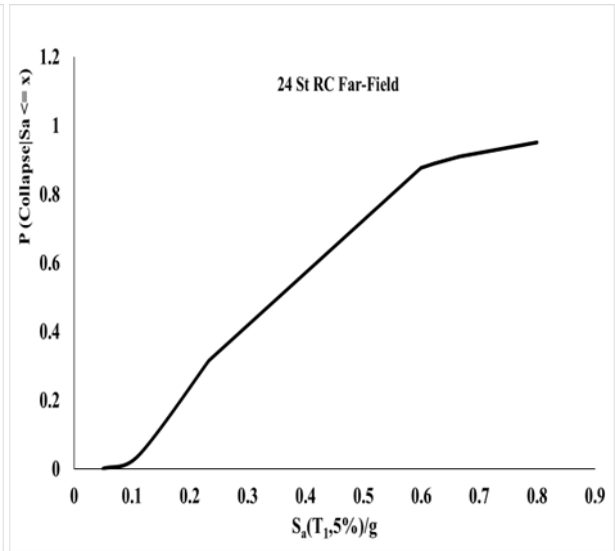


Figure 10. Fragility curves of 24-story model for far-field records.

6.2. Results of IDA for Near-Field Records

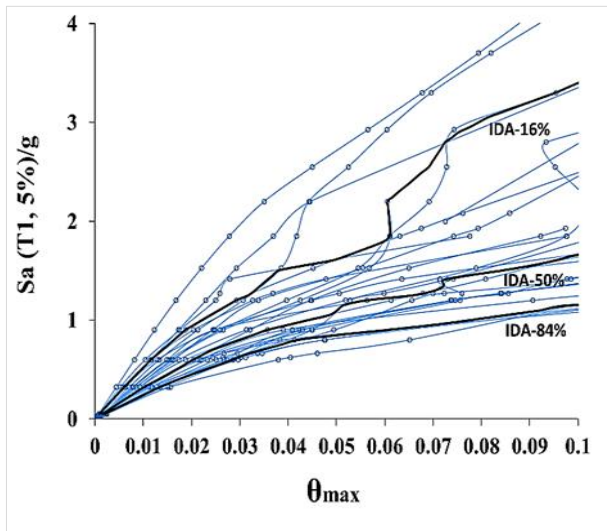


Figure 11. IDA curves of 4-story model for near-field records with pulse.

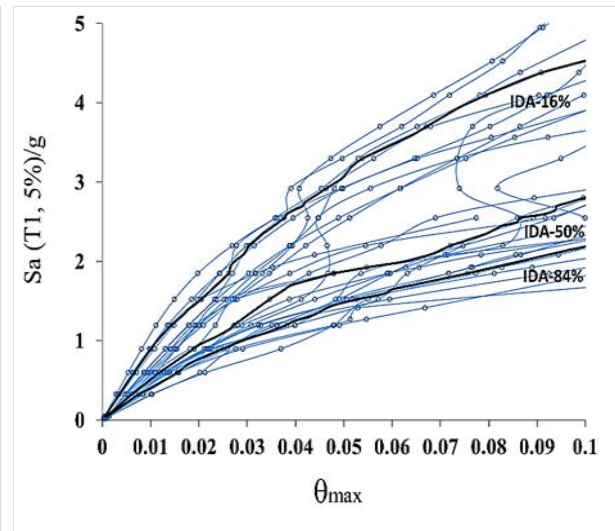


Figure 12. IDA curves of 8-story model for near-field records with pulse.

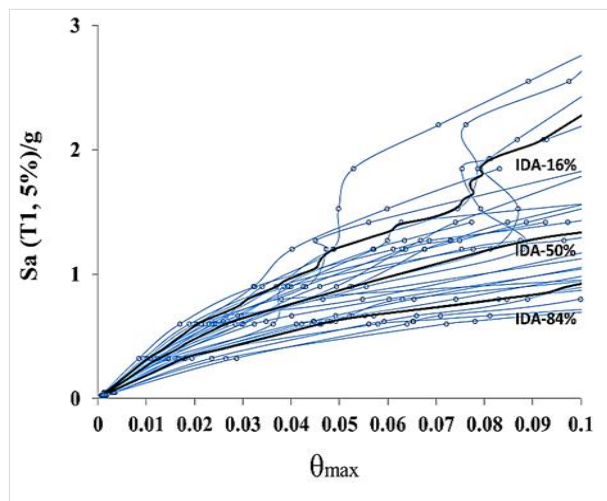


Figure 13. IDA curves of 12-story model for near-field records with pulse.

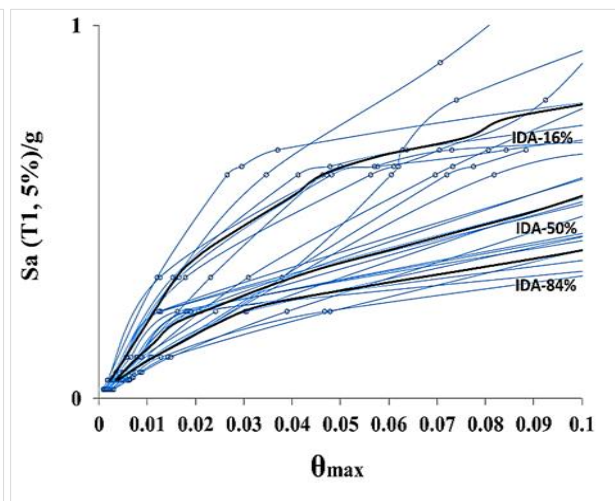


Figure 14. IDA curves of 24-story model for near-field records with pulse.

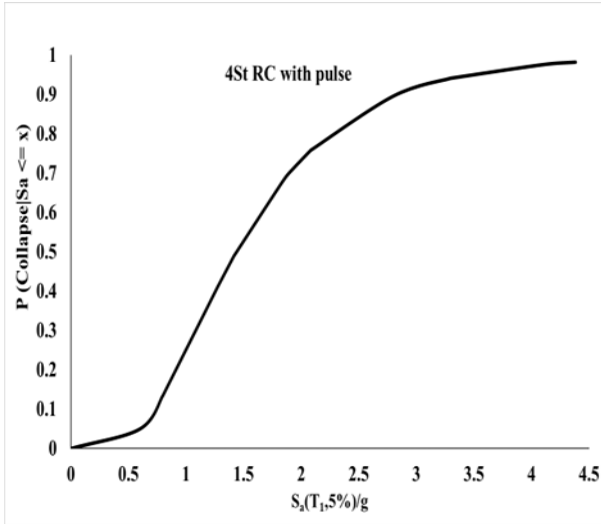


Figure 15. Fragility curves of 4-story model for near-field records with pulse.

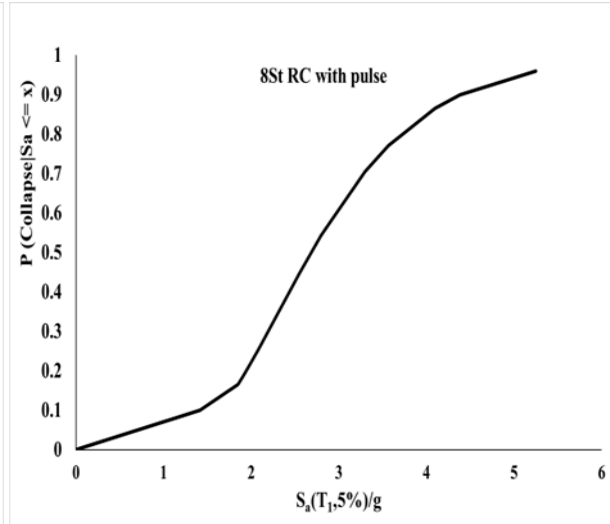


Figure 16. Fragility curves of 8-story model for near-field records with pulse.

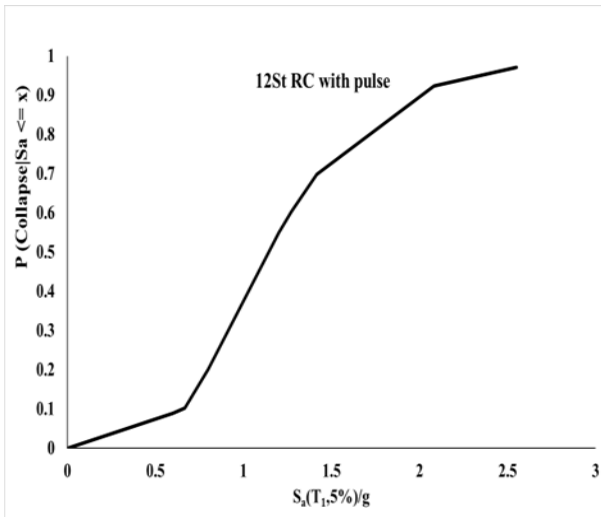


Figure 17. Fragility curves of 12-story model for near-field records with pulse.

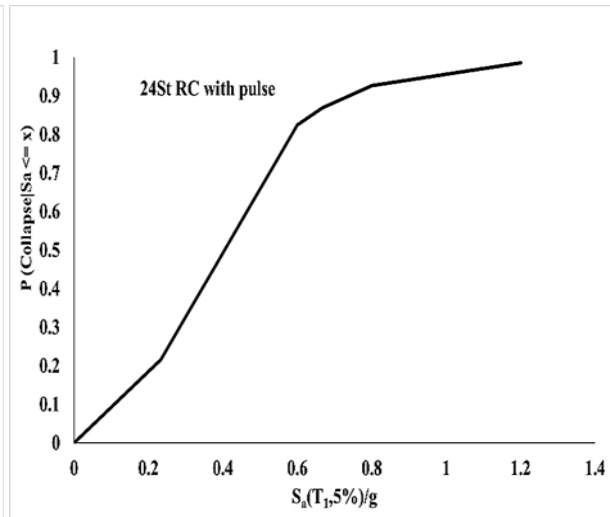


Figure 18. Fragility curves of 24-story model for near-field records with pulse.

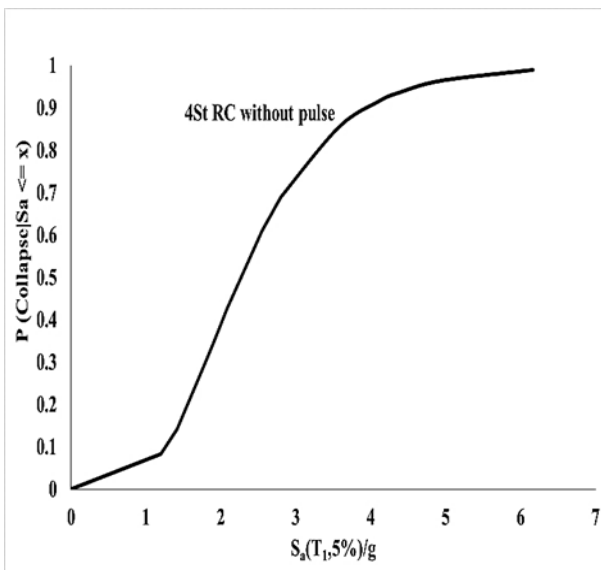


Figure 19. Fragility curves of 4-story model for near-field records without pulse.

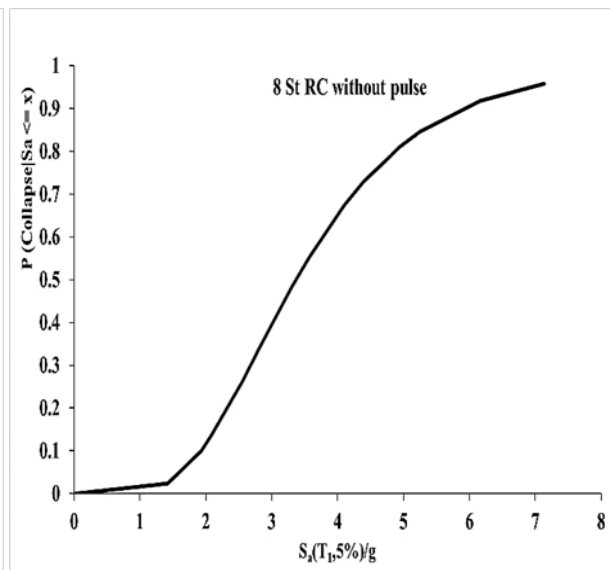


Figure 20. Fragility curves of 8-story model for near-field records without pulse.

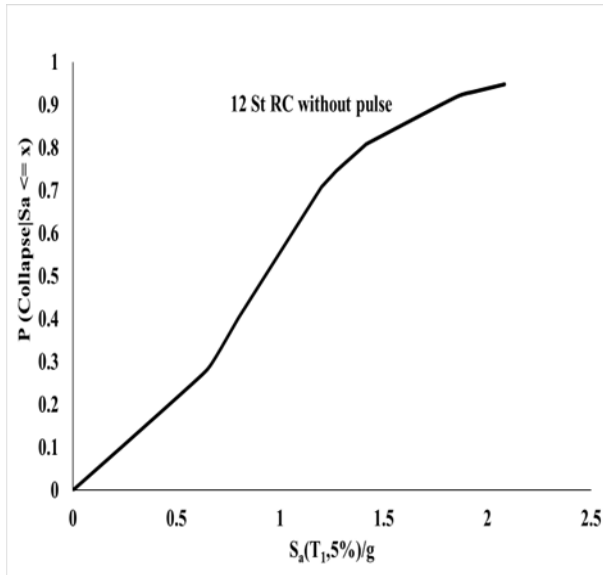


Figure 21. Fragility curves of 12-story model for near-field records without pulse.

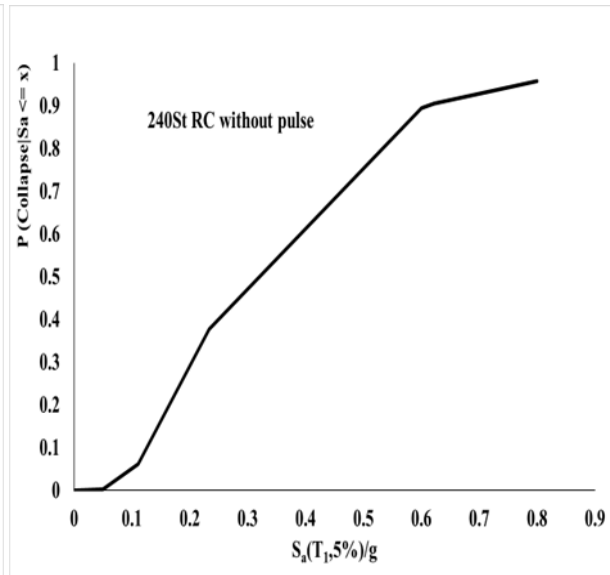


Figure 22. Fragility curves of 24-story model for near-field records without pulse.

7. Fragility curves and total uncertainty of the structure

According to the proposed method of FEMA-P695 and using the provided relations, the collapse of the models designed with the 2800 standard of Iranian earthquake was evaluated. The overall uncertainty of the structure is calculated according to the equation (1) of FEMA-P695.

$$\beta_{TOT} = \sqrt{\beta_{RTR}^2 + \beta_{DR}^2 + \beta_{TD}^2 + \beta_{MDL}^2} \quad (1)$$

Where $\beta_{RTR}, \beta_{DR}, \beta_{TD}, \beta_{MDL}, \beta_{TOT}$ represent the uncertainties of the selected records, design, experimental information, modelling, and general uncertainty of the structure, respectively. Differences in the response of the structures under different earthquake records can be attributed to differences in the frequency content and different dynamic properties of earthquake records. According to research conducted by Hasleton (2006), Ibarra and Kravinkler (2005), and Zareian et al. (2006), it can be stated that the amount of uncertainty related to selected records (β_{RTR}) for different building systems is about 0.35 to 0.45. Equation (2) relates the amount of uncertainty in association with the set of earthquake records to the ductility coefficient of the structure.

$$\beta_{RTR} = 0.1 + 0.1\mu T \leq 0.4 \quad (2)$$

8. Assessing the collapse of the structure

To evaluate the collapse of the structure, first, the ACMR parameter is calculated according to the spectral shape correction factor (SSF) and also the CMR parameter and is compared with similar values in the FEMA-P695 instruction [4] (Tables 2-5). Spectral acceleration in the first mode of the structure for an earthquake with a return period of 2475 years is the same as the Maximum Credible Earthquake (MCE) surface earthquake (Figure 23) [13].

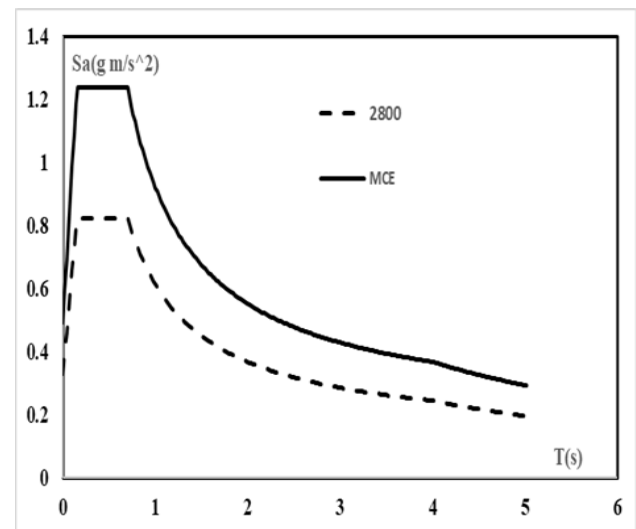


Figure 23. 2800 spectrum and maximum possible MCE earthquake [13]

Table 2: Effective parameters in assessing the safety margin of the modified collapse and evaluating the performance of the 4-story model.

Seismic Records	S_CT	S_MT	CMR	SSF	ACMR	Accepted ACMR	Percent increase of ACMR	Performance
Far-field	1.88	1.13	1.66	1.11	1.84	1.62	14%	Accepted
Near-field without pulse	2.27	1.13	2.01	1.11	2.23	1.66	34%	Accepted
Near-field with pulse	1.44	1.13	1.27	1.11	1.41	1.66	-15%	Not accepted

Table 3: Effective parameters in assessing the safety margin of the modified collapse and evaluating the performance of the 8-story model.

Seismic Records	S_CT	S_MT	CMR	SSF	ACMR	Accepted ACMR	Percent increase of ACMR	Performance
Far-field	2.8	1.1	2.55	1.1	2.81	1.66	69%	Accepted
Near-field without pulse	3.37	1.1	3.06	1.1	3.37	1.66	103%	Accepted
Near-field with pulse	2.69	1.1	2.45	1.1	2.70	1.66	63%	Accepted

Table 4: Effective parameters in assessing the safety margin of the modified collapse and evaluating the performance of the 12-story model.

Seismic Records	S_CT	S_MT	CMR	SSF	ACMR	Accepted ACMR	Percent increase of ACMR	Performance
Far-field	1.03	0.76	1.36	1.22	1.66	1.66	0%	Accepted
Near-field without pulse	0.93	0.76	1.22	1.22	1.49	1.66	-10%	Not accepted
Near-field with pulse	1.14	0.76	1.50	1.22	1.83	1.66	10%	Accepted

Table 5: Effective parameters in assessing the safety margin of the modified collapse and evaluating the performance of the 24-story model.

Seismic Records	S_CT	S_MT	CMR	SSF	ACMR	Accepted ACMR	Percent increase of ACMR	Performance
Far-field	0.35	0.60	0.58	1.32	0.77	1.66	-54%	Not accepted
Near-field without pulse	0.32	0.60	0.53	1.32	0.70	1.66	-58%	Not accepted
Near-field with pulse	0.40	0.60	0.67	1.32	0.88	1.66	-47%	Not accepted

9. Conclusion

In this research, Reinforced Concrete Frame structures are modelled and in order to perform nonlinear incremental dynamic analysis of FEMA-P695 recommended far and near-field records, were selected. In the discussion of fragility curves and probability of failure, it seems that the performance of special reinforced concrete is acceptable in low and mid structures and unacceptable in high-rise structures.

Funding Statement

This research received no external funding.

Data Availability

The data used to support the findings of this study are included within the article.

Conflicts of Interest

The author declare that there is no conflict of interest regarding the publication of this paper.

References

- [1] Kennedy, R. P.; Cornell, A. C. Campbell, R. D. Kaplan, s. and Parla, H.f. (1980). "Probabilistic seismic safety study of an existing nuclear power plant", Nuclear Eng and Design,59(2).
- [2] Anagnos, T.; Rojahn, C. and Kiremidjian, A. S. "Building fragility relationship for California", Proceeding of the Fifth U. S. National Conference on Earthquake Engineering, pp.389-396(1994).
- [3] J. Shin, J. Kim, K. Lee, Seismic assessment of damaged piloti-type RC building subjected to successive earthquakes, Earthquake Engineering & Structural Dynamics, 43(11) 1603-1619 (2014).
- [4] FEAMAP695.; P695-Quantification of Building Seismic Performance Factors, Federal Emergency Management Agency (FEAMA)"; Document No (2009), F fama.
- [5] Choi, I. and Park, H" Cyclic Loading Test for Reinforced Concrete Frame with Thin Steel Infill Plate" J. Struct. Eng., 137(6), 654–664 (2011).
- [6] Mazzoni, S., et al.; "OpenSees command language manual"; Pacific Earthquake Engineering Research (PEER) Center (2006).
- [7] Stafford Smith, Alex Coull, Translate by haji kazemi," Tall Building".' In: Tall Building Structures: Analysis and Design (In Persian) (1991).
- [8] Iranian National Building Code. Applied Loads on Buildings. Part 6, Ministry of Roads & Urban Development: Tehran, Iran, 2013.
- [9] Iranian National Building Code. Design and Implement of Concrete Buildings. Part 9, Ministry of Roads & Urban Development: Tehran, Iran, 2013.
- [10] I.S. Code, Iranian Code of Practice for Seismic Resistant Design of Buildings 2800., 4th ed Ministry of Roads & Urban Development: Tehran, Iran, 2014.
- [11] Rouhi, H., & Gholhaki, M, Nonlinear behavior of reinforced concrete frames equipped with and without steel plate shear wall under sequence of real and artificial earthquakes, Advances in Civil Engineering, pp 1–26 (2022). Article ID 9512286.
- [12] Vamvatsikos, D. and Cornell. C.A "Incremental dynamic analysis," Earthquake Engineering. And Dynamic structures, 31(3), pp 491-512., (2002).
- [13] Rouhi, H, and Gholhaki, M. "Investigation of Seismic Vulnerability of Reinforced Concrete Frames Equipped with Steel Plate Shear Walls", Engg. Research: Online First Article (2022).



Open Access This article is licensed under a Creative Commons Attribution 4.0 International License, which permits use, sharing, adaptation, distribution and reproduction in any medium or format, as long as you give appropriate credit to the original author(s) and the source, provide a link to the Creative Commons license, and indicate if changes were made. The images or other third-party material in this article are included in the article's Creative Commons license, unless indicated otherwise in a credit line to the material. If material is not included in the article's Creative Commons license and your intended use is not permitted by statutory regulation or exceeds the permitted use, you will need to obtain permission directly from the copyright holder. To view a copy of this license, visit <https://creativecommons.org/licenses/by/4.0/>.

© The Author(s) 2023